

Bio-harmonized Dynamic Model of a Biology Inspired Carangiform Robotic Fish Underwater Vehicle^{*}

Abhra Roy Chowdhury^{*} Bhuneshwar Prasad^{*}
Vinoth Vishwanathan^{*} Rajesh Kumar^{**} S K Panda^{*}

^{*} *Department of Electrical and Computer Engineering, National
University of Singapore, Singapore 117576 (Tel: 6516-5257; Email:
abhra.roychowdhury@nus.edu.sg)*

^{**} *Electrical Engineering Department, Malviya National Institute of
Technology, Jaipur, India*

Abstract: This paper presents a novel dynamic model of a bio-inspired robotic fish underwater vehicle by unifying conventional rigid body dynamics and bio-fluid-dynamics of a carangiform fish swimming given by Lighthill's (LH) slender body theory. It proposes an inclusive mathematical design for better control and energy efficient path travel for the robotic fish. The system is modeled as an 2-link robot manipulator (caudal tail) with a mobile base (head). Lighthill caudal-tail reactive forces and moments are shown to contribute towards thrust generation and yaw balance. These LH reactive forces are shown to generate the inertial added mass during the robotic fish locomotion. This forward thrust drives the robotic fish head represented by a unified non-linear equation of motion in earth fixed frame. Using the proposed dynamic model an open-loop (manual) operating region for the identified kinematic parameter tail beat frequency (TBF) is established. Obtained Kinematic results also resemble with real fish kinematic results. The objective is to mimic the propulsion technique of the carangiform swimming style and to show the fish behavior navigating efficiently over large distances at impressive speeds and its exceptional character in fluid environment.

Keywords: Biology-inspired Robotics, Carangiform, Lighthill Slender Body theory, Dynamics Modeling, Kane's method.

1. INTRODUCTION

Exploring the spatial locomotion of certain aquatic vertebrates that are able to travel at surprisingly remarkable speeds, has been the interest of researchers towards the contribution of the bio-inspired robotics [1]. Biomimetics reflect the features and capabilities of natural evolution of a system that could be efficiently mimicked or harmonized in a human engineered system to design of new technologies and improvement of conventional ones in terms of propulsion efficiency. One of the focused technologies has been the development of autonomous underwater vehicles [2] to the increasing interest in unmanned underwater surveillance and monitoring. The propeller based locomotion [2] although rendered the initial answers to underwater locomotion but it sets issues on high-maneuverability and efficiency. The researchers also found that propeller-strikes produce greater amount of marine debris, marine creatures mortality and shallow waters ecosystem disturbances. Bio-harmonized fish-like robots are expected to be

quieter, more maneuverable (lesser accidents), and possibly more energy efficient (longer missions).

Theoretical and experimental validations of the dynamic equations of motions for underwater vehicles are mentioned in Fossen [4] pointing on the advantages of Lagrangian framework over Newtonian approach. The vehicle-manipulator system dynamic model in closed loop is investigated in Schjølberg [5] where the hydrodynamic forces are included in the Newton-Euler framework. Tarn [6] employs Kane's method combining the advantages of both Newton and Lagrange's techniques to develop a dynamic model of yet another vehicle-manipulator system. It shows a direct method to include the hydrodynamic forces as generalized inertial forces in the system's governing equations of motion. The systems discussed above were driven by conventional propellers. Biomimetic carangiform [3] fish like propulsion or non-propeller systems have been studied since the early works of MIT's robot tuna[8]. Robotic fish motion as a 2-link (open chain) manipulator model and its control based on passive dynamics was reported by Nakashima [7]. Many researchers have developed Lagrange and Newton based dynamic modeling with innovative schemes of force transmission like using tendon based mechanism [8] or passive components [7] to mimic the tail muscle agility. The systems considered in these research reports are open chain serial manipulators with

^{*} This work is presently supported by the Defence Science and Technology Agency (DSTA), under the Ministry of Defence (Singapore), Government of Singapore, under Grant R-263-000-621-232-MINDEF-DSTA for Underwater Vehicle Technology Project STARFISH 2.

1 DOF rotational joints and a mobile base. Yu [9] used Schiehlen method to formulate a cetacean inspired three-dimensional multibody dynamics model. In these works [7,8,9] including [19,20], Lighthill's (LH) slender body theory waveform [10] produces posterior body undulations (lateral displacements) necessary for thrust generation. But the pressure forces reported in Lighthill [13] were not completely integrated in the dynamics. This gap was addressed by J. Wang [11] who presented a new dynamic model for a carangiform robotic fish by merging rigid-body dynamics with Lighthill's large-amplitude elongated-body theory [12]. The system is 14 cm long (including the tail) and 8 cm wide with one joint link acting as the oscillating tail-fin as compared to the present robotic fish which is 74 cm in length, and weighs 4.5 kg. Boyer et al.[18] also proposed a dynamic model on the later theory and on-line control of a more adept bio-mimetic anguilliform eel-like robot. Under the LH slender body framework [10] RoyChowdhury et al. [20,21] studied the major kinematic parameters and showed that a shorter path is travelled by the robotic fish using Lighthill bio-inspired algorithm.

The contributions of the present research are enumerated as following:

- Develop a carangiform fish-biology-harmonized inspired-dynamic model under Lighthill's slender body theory framework. The resulting nonlinear equations of motion are expressed in terms of dominant kinematic parameters i.e. tail-beat frequency (TBF), the propulsive wavelength and the caudal amplitude in open-loop (manual).
- Define an unified dynamic model of robotic fish in earth fixed coordinate merging the conventional rigid body dynamics and bio-fluid-dynamics given by Lighthill reactive theory together to justify the fish-like efficient swimming. The robotic fish head is the mobile base and an n -link manipulator resembling caudal tail acts as a propeller, generating thrust by periodic undulatory motion.
- Formulate caudal-tail dynamics using Kane's method to exploit the benefits of Lagrange and Newtonian methods.
- Examine the effects of kinematic parameters on the overall system dynamics.
- Establish an operating region for the robotic fish vehicle based on the identified major kinematic parameters i.e. TBF vis a vis the real biological yellowfin tuna kinematics to facilitate an open-loop (manual) control.
- Demonstrate the feasibility of real time flexible bodied robotic fish vehicle prototype propelled by a n -joint oscillating caudal fin under the proven Lighthill Slender body theory.

The rest of the paper is organized as follows. In Section II, the dynamics modeling of a three link robotic fish is discussed. Subsection A discusses the rigid body equations of motion of the anterior or head while subsection B defines the dynamic model of the posterior 2-link caudal tail employing Kane's method. This section also expresses two types of Lighthill's slender body theory bio-fluid-dynamics forces. Finally, a unified force balance equation is written for the robotic fish vehicle prototype in earth fixed coordinate. Section III presents the simulation and

experimental results obtained based on existing dynamic model and existing kinematic analysis [20] of the robotic fish. Forward swimming velocity is plotted as a function of kinematic parameter TBF. Based on the experiments, an operating region is found for the dominating parameter TBF for various conditions of body wavelength. In Section IV, conclusions and directions for future work are discussed.

2. SYSTEM MODEL

This paper proposes the bio-inspired underwater robotic-fish as a three link system manipulator such that its geometric shape mimics the structure of a carangiform fish. The first link or the head is considered as a mobile base while the two serially connected links (using rotational joints) or caudal tail are considered to act as thruster using their coordinated undulatory lateral displacements (perpendicular to the plane of motion). Inspired by the biological fish swimming fluid-dynamics model mentioned in Lighthill slender body theory, the present robotic fish dynamic modeling integrates bio-mechanics as the reactive pressure forces and their moments. These occur due to the lateral undular displacements of caudal tail. This integration can be justified on the fact that a biologically inspired propulsion and its associated dynamics have to be redefined if compared to the conventional underwater vehicle-manipulator systems using propeller based thrust generation. As shown in Fig.1 a kinematics model of Robotic-fish, with coordinated motion of multiple propulsive mechanisms, is drawn using CAD design tool SolidWorks and imported to MATLAB through a common data exchange interface.

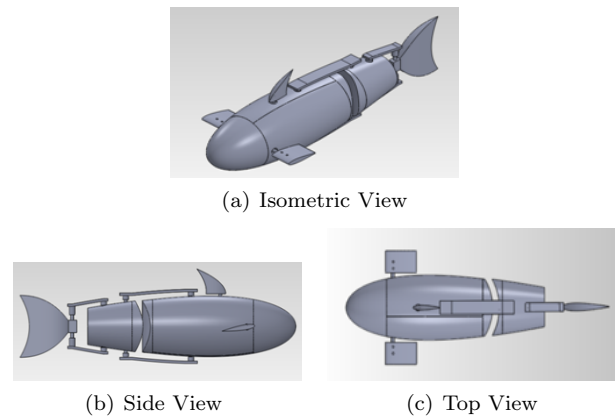


Fig. 1. Solidworks Robotic Fish Model

The entire robotic fish body cannot be considered as a single rigid body as it eliminates the consideration of reaction forces acting between individual body links. Therefore a modular modeling technique has been used to give the unified model for the entire vehicle system. While the anterior employs Fossen's [4] Lagrangian's method, the posterior two-link caudal tail uses Kane's Method [15] for the equations of motion. Derivation of interactive and constraint forces between the two bodies is excluded by expressing the generalized forces.

2.1 Robotic Fish (Anterior) Head

Robotic fish head carries maximum hotel-load as most of the electronic circuits including battery pack and ballast are located in it. It is assumed to be a prolate ellipsoid shape. Defining the dynamics of the robotic fish head is based on standard Lagrangian formulation given by Fossen [4]. While the kinematics study explain the geometry of the motion of robotic fish wrt a fixed reference coordinate frame as a function of time, the dynamics of any rigid body [8] can be completely described by the translation of the centroid and the rotation of the body about its centroid.

Therefore, the vehicle's three translational (f_0) and three rotational (m_0) motions derived from the momentum conservation laws defined in usual notations mentioned in Fossen [4] (for a rigid body of mass constant m and centre of gravity r_G) are expressed as:

$$m(\dot{v}_0 + \omega \times v_0 + \dot{\omega} \times r_G + \omega \times (\omega \times r_G)) = f_0 \quad (1)$$

$$I_0(\dot{\omega} + \omega \times (I_c \omega)) + m r_G (\dot{v}_0 + \omega \times v_0) = m_0 \quad (2)$$

which further can be expressed in

$$M_h(\eta)\ddot{\eta} + C_h(\nu, \eta)\dot{\eta} + D_h(\nu, \eta)\dot{\eta} + g_h(\eta) = \tau_h \quad (3)$$

where M_h is the head inertia matrix including the added inertia, C_h is the Coriolis-centripetal matrix, g_h is the gravity matrix, τ_h is the propulsion forces vector, η is position and orientation vector $[x, y, z, \phi, \theta, \psi]$ in earth fixed coordinate and ν is linear and angular velocity vector $[u, v, w, p, q, r]$ in body fixed coordinate [4].

2.2 Robotic Fish (Posterior) 2-Link caudal tail/Thruster

The *BCF* mode carangiform style [2] of locomotion is approximated using a 3-link (including the pectorals attached to the head) mechanism with two actuated joints as shown in Fig.2. This leads to the ability to derive the actuator torques necessary to produce the tail motion that is desired. The links are inter-dependent in two major respects:

- The torque produced by a link produces a reaction torque on the other links.
- The motion of the links changes the shape of the linkage and thereby the inertia seen by previous links.

A linearized kinematic and dynamic model of the robotic fish system is developed. The coordinate frames in which the overall vehicle moves is with respect to the earth fixed frame. This frame is obtained from a body fixed reference frame shown in Fig.2. When describing the kinematics and dynamics of 2-Link caudal tail model, the interlink actuator-shaft constitutes the inertial frame of reference. A local coordinate frame is assigned to each DOF detailed as below.

(a) Reference Frames:

- F_I : inertial frame of manipulator-base system.
- F_B : base Frame located at the centre of mass of the base.
- F_i : coordinate frame of the i_{th} link of the manipulator

(b) Vectors:

- r_B : position of frame F_0 relative to and projected onto frame F_B .

- r_I : position of frame F_0 relative to and projected onto frame F_O .
- p_i : position of point on link i relative frame F_i .

Using the standard *Denavit-Hartenberg* [16] convention, the final transformation of caudal-tail fin with respect to the head (first link) in earth fixed frame is given by:

$${}^0A_2 = {}^0A_1^1A_2 \quad (4)$$

where the transformation matrix for $i = 1, 2$ is given by

$${}^iA_{i-1} = \begin{bmatrix} c\theta_i & -s\theta_i & 0 & l_i c\theta_i \\ s\theta_i & c\theta_i & 0 & l_i s\theta_i \\ 0 & 0 & 1 & 0 \\ 0 & 0 & 0 & 1 \end{bmatrix}$$

2.2.1 Velocity and Acceleration vectors : As mentioned head or the first link is taken as a reference coordinate for the subsequent link frames. The position vectors of the Centre of Mass (*COM*) for the 2-link (caudal-tail) w.r.t first link (head) coordinate in inertial frame can be expressed as

$${}^0p_i = {}^0r_0 + {}^0A_1^1r_i \quad (5)$$

where $i = 1, 2$ denoting two link numbers. The angular and linear velocity vector derived in inertial frame w.r.t first link becomes:

$${}^0\omega_i = {}^0\omega_i + {}^0\theta_i \cdot {}^0z_i \quad (6)$$

$${}^0v_i = {}^0v_i + {}^0\omega_i \times {}^0p_i \quad (7)$$

The angular and linear acceleration vector derived in inertial frame w.r.t first link can be written as:

$${}^0\alpha_i = {}^0\dot{\omega}_i + {}^0\omega_0 \times {}^0\omega_i \quad (8)$$

$${}^0a_i = {}^0\dot{v}_{i-1} + {}^0\omega_0 \times {}^0v_i \quad (9)$$

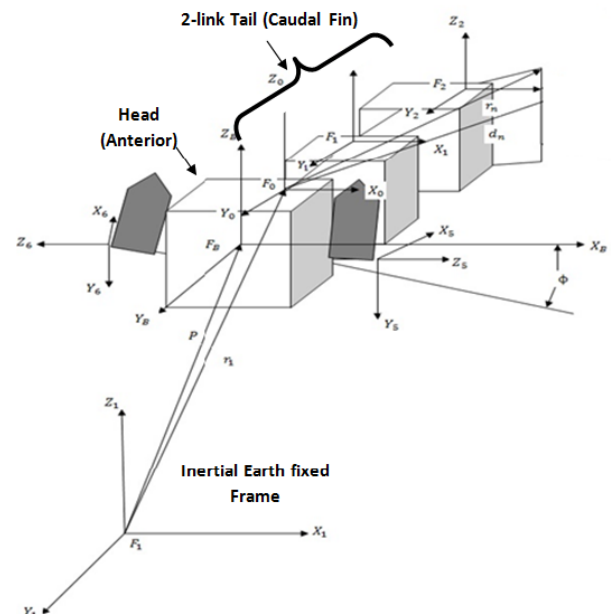


Fig. 2. Relative orientations and locations of local coordinate frames at the CM of the head and the Inertial reference frame

2.2.2 Forces and Torques : The inertia forces and torques associated to the respective links are given by:

$$\text{ReactionForce} : R_i = -m_i^0 a_i \quad (10)$$

$$\text{Torque} : T_i = -{}^0 I_i^0 \alpha_i - {}^0 \omega_i \times {}^0 I_i^0 \omega_i \quad (11)$$

Therefore, the generalized forces and torques [6, 15] for both links can be expressed as

$$F_i = \sum_{i=1}^2 \left(\frac{\partial^0 \omega_i}{\partial \dot{\theta}_i} \cdot T_i + \frac{\partial^0 v_i}{\partial \dot{\theta}_i} \cdot R_i + m_i \frac{\partial^0 v_i}{\partial \dot{\theta}_i} \cdot g \right) \quad (12)$$

where $g = -9.8 \text{ m/sec}^2$

2.2.3 Hydrodynamic Forces: Added Mass (Lighthill's Reactive Force) A submerged rigid body motion would result in nonlinear hydrodynamics forces acting on it. These are complex forces to numerically integrate into a model which has also led to semi-empirical modeling techniques [17]. Added Mass [4,10] is a combination of pressure induced forces and moments resulting due to the inertia of surrounding fluid around the two-links, which are in acceleration motion w.r.t the fluid. Lighthill slender body theory [10] considers a fish doing swimming movements in inviscid fluid flowing with velocity U in the x -direction. The body cross-section, would receive a displacement $h(x,t)$ in the transverse/lateral z -direction varying both in time and position causing a flow due to it. $h(x,t)$ [10] depicts the lateral push of vertical water section by the successive cross sections past which it sweeps with velocity U . It is the mathematical form given below, physically denoting undulatory mode of carangiform propulsion in which a transverse travelling wave of increasing amplitude is generated from anterior to posterior of body.

$$h(x,t) = f(x)g(t - x/c) \quad (13)$$

For the present robotic fish a quadratic spline mathematical form [8,20,21] is used as

$$h(x,t) = y_{body}(x,t) = [(c_1 x + c_2 x^2)][\sin(kx + \omega t)] \quad (14)$$

where caudal amplitude, c_1 and c_2 are calculated parameters based on real fish kinematics while TBF, ω range is found from simulation [20]. Lateral velocity $w(x,t)$ [10] resulting due to it can be written as

$$w(x,t) = \frac{\partial h}{\partial t} + U \left(\frac{\partial h}{\partial x} \right) \quad (15)$$

where U is the mean speed. For the 2-link system it [19] is found to be

$$U = l_1 \frac{d}{dt}(\theta_1) \cos \theta_1 + a_2 \frac{d}{dt}(\theta_2) \cos \theta_2 \quad (16)$$

Substituting $h(x,t)$ we obtain lateral velocity to be

$$w(x,t) = f(x) \frac{d}{dt}g(t - x/c)(Uk + \omega) + \frac{d}{dt}f(x)g(t - x/c) \quad (17)$$

As the fish undulates, lateral velocity is transformed in to linear and angular momenta [10] which is shed by caudal fin added mass (two-links) into water results in lateral push or in other terms pressure forces and their moments. These contribute to both the thrust production and side-force generated imbalances in yaw-movement [13]. The lateral momentum is represented as

$$L(x,t) = \rho \left(\frac{\partial h}{\partial t} + U \frac{\partial h}{\partial x} \right) w(x,t) \cdot S_x \quad (18)$$

The swimming efficiency of fishes is found to be caused by a two way technique adopted by the fish i.e. linear and angular momentum conservation laws. The resulting forces and moments responsible are classified into two types namely the thrust (longitudinal) P and the side force balancing(lateral) Q . As both the forces/moments are caused due to the reaction of added mass of the caudal tail's (two-links's) inertia/inertance and not its resistance in fluid, they are called reactive forces. Lighthill [10,12,13] further adds that the advantage of a piscean design allows significant reactive forces on the caudal cross section to contribute to the overall thrust and minimize the recoil. In carangiform, reactive forces are dominant as the acceleration of water (virtual mass) in contact with the body surface happens fast as compared to resistive forces which take longer time to build up during the overall lateral displacement. Present model uses NACA 0014 airfoil design i.e. a pronounced reduction in body cross-sectional depth along the posterior caudal region to contain the morphological feature of the carangiform thereby supporting the reactive force theory [13]. In Fig.3 the two links (shown by two lines) are considered to be in the continuum mechanics of a fish spinal column. Fish is assumed to be swimming in horizontal x -axis and with a lateral y -axis in the same plane while z -axis is vertical. Using a lagrangian coordinate [11,12] a along the length of the fish spinal chord we assume two points $x(a,t)$ and $y(a,t)$ (marked by black dots) on the posterior two links separately (caudal fin) on which the LH undulatory wave is generated. The points will move with undulatory motion i.e. a lateral recoil displacements/ motions and a resultant forward translation motion.

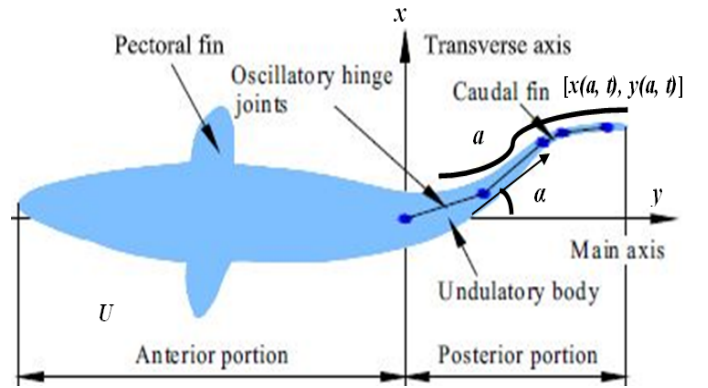


Fig. 3. Model of Carangiform Swimming showing the undulation motion in 2/3rd part on the spinal column and lagrangian coordinates

Assuming inextensibility of spinal column [12] as the entire design can be seen as an ellipse with minor axis in the z -direction,

$$\left(\frac{\partial x}{\partial a} \right)^2 + \left(\frac{\partial y}{\partial a} \right)^2 = 1 \quad (19)$$

Here $\frac{\partial y}{\partial a}$ is the cosine of the angle between caudal fin and the mean swimming direction which is also called as the angle of attack" α "

$$\left(\frac{\partial y}{\partial a} \right) = \cos(\alpha); \left(\frac{\partial x}{\partial a} \right) = \sin(\alpha) \quad (20)$$

Tangential motion, as the horizontal component of the velocity $\left(\frac{\partial x}{\partial t}, \frac{\partial z}{\partial t} \right)$ is given by

$$u_L = \left(\frac{\partial x}{\partial t} \frac{\partial x}{\partial a} + \frac{\partial y}{\partial t} \frac{\partial y}{\partial a} \right) \quad (21)$$

Transverse motion is then given by:

$$w_L = \left(\frac{\partial x}{\partial t} \frac{\partial y}{\partial a} - \frac{\partial y}{\partial t} \frac{\partial x}{\partial a} \right) \quad (22)$$

It is to be noted that the tangential motions would be treated resistively while transverse motions would be taken care of by reactive forces. The resistive forces are similar to pressure/profile drag forces and would be modeled in later section for the two links.

a) Reactive Thrust force P

From the conservation of momentum laws we define the transverse movements force component Z [13] in y -direction with which 2-link fish-caudal of virtual mass m per unit length, pushes the water slice with lateral velocity w , per unit distance in x -direction

$$Z = m \left(\frac{\partial}{\partial t} w(x, t) + U \frac{\partial}{\partial x} w(x, t) \right) \quad (23)$$

which can also be written after substituting suitably from equations (16),(17) and (18)

$$Z = -m\omega \left[h(x, t)(Uk + \omega) - \dot{f}(x) * \dot{g}(t - x/c) \right] \quad (24)$$

The rate of work done E [13] by fish by producing the undulatory transverse movement with a force Z is given by

$$E = \int_0^l Z \frac{\partial h}{\partial t} dx \quad (25)$$

From the equation relating work done and thrust P , we derive the thrust equation given by

$$P = \left[mw \left(\frac{\partial x}{\partial t} - 0.5w \cos \alpha \right) \right]_{a=0} - \frac{d}{dt} \int_0^l mw \sin \alpha da \quad (26)$$

The term consisting of variable product "mw" or lateral momentum explains mean power or thrust used by the fish tail in lateral push near the trailing edge. The first term represents the body's exchange of energy with water during motion in y direction. Putting the value of $h(x, t)$ and U in this equation, the final expression of forward thrust in fourier series form can be derived as

$$P = m[P_1(\Lambda) \sin(\omega t + kx + \alpha) + P_2(\Lambda) \cos(\omega t + kx + \alpha)] \quad (27)$$

where $\Lambda = [\omega, U, k, c_1, c_2, x]$ which resembles the fourier form of force equation mentioned in Lighthill [13]. therefore functions P_1 and P_2 can be seen as the force components as a function of kinematic parameters $\omega, U, (\theta_1, \theta_2), c_1, c_2$ [20,21].

b) Reactive Side force

The side-force [13] is given by the expression

$$Q = - \left[mw \left(\frac{\partial y}{\partial t} + 0.5w \frac{\partial x}{\partial a} \right) \right]_{a=0} + \frac{d}{dt} \int_0^l mw \frac{\partial x}{\partial a} da \quad (28)$$

$$Q = - \left[mw \left(\frac{\partial y}{\partial t} + 0.5w \sin \alpha \right) \right]_{a=0} + \frac{d}{dt} \int_0^l mw \cos \alpha da \quad (29)$$

This side-force is important as the balance of its fluctuations indicate recoil losses (unbalanced oscillations) which in turn are associated to the yaw motion and sideslip. Putting the value of $h(x, t)$ and U in this equation the final form appears to be once again in fourier series form given by

$$Q = m[Q_1(\Lambda) \sin(2\omega t + \alpha) + Q_2(\Lambda) \cos(2\omega t + \alpha)] \quad (30)$$

where $\Lambda = [\omega, U, k, c_1, c_2, x]$ The role of α or angle of attack in above equations of P and Q derived term is imminent and would be a topic of study in future work. Based on above total thrust force and total side-force can be written as

$$F_{lh} = \int_0^l \left(P + m \frac{\partial^2 h}{\partial t^2} \right) dx \quad (31)$$

Moment of side-force is given by

$$M_{lh} = \int_0^l \left((l-x) \times \left(Q + m \frac{\partial^2 h}{\partial t^2} \right) \right) dx \quad (32)$$

Suitable to be used in numerically integration with other forces as well as from the control design point aspect a matrix form of the force and moment equations could be written as:

$$\begin{bmatrix} F_{lh} \\ M_{lh} \end{bmatrix} = \begin{bmatrix} P_1(\Lambda) & P_2(\Lambda) \\ Q_3(\Lambda) & Q_4(\Lambda) \end{bmatrix} \begin{bmatrix} \sin(a\omega t + b\alpha) \\ \cos(a\omega t + b\alpha) \end{bmatrix}$$

where $a, b \in Z$

Generalized Lighthill inertia force is therefore given by

$$F_{LH} = \sum_{i=1}^2 \left(\frac{\partial^0 \omega_i}{\partial \theta_t} \cdot F_{lh} + \frac{\partial^0 v_i}{\partial \theta_t} \cdot M_{lh} \right) \quad (33)$$

2.2.4 Buoyancy Force : Buoyancy [4] is a restoring force proportional to the displaced amount of fluid mass by the weight of two links. Here we consider that the centre of buoyancy and COM coincide as the geometry shows symmetry. The two links would experience a generalized buoyancy force given by:

$$F_b = \rho \sum_{i=1}^2 \left(V_i \frac{\partial^0 v_i}{\partial \theta_t} \cdot g \right) \quad (34)$$

2.2.5 Pressure Drag (Resistive) Force : Lighthill [10] mentions Gray's conclusion that major objective of overcoming drag in powered swimming requires fishes to generate thrust. Typically the fish (caudal and pectoral) fins have been designed and modeled by nature to maintain optimum pressure distribution i.e. fin surface energy, maintaining laminar flow, minimizing total flow pressure and reduced drag. The fish undulation provides high thrust rates and therefore efficient movement in fluids. The pressure drag (resistive force) is proportional to the square of velocity, projected cross-sectional area, fluid density and drag coefficient C_d . The inertia forces and moments caused therefore are expressed as

$$R_{di} = -0.5\rho \int_{i=1}^2 \|\dot{v}_i(l)\|^0 \dot{v}_i(l)^\perp C_d b_i dl \quad (35)$$

$$T_{di} = -0.5\rho \int_{i=1}^2 \|\dot{v}_i(l)\|^0 A_i l \times^0 \dot{v}_i(l)^\perp \times C_d b_i dl \quad (36)$$

The value of drag coefficient C_d for the present robotic fish is computed through CFD studies and experimentally validated to a real carangiform fish hydrodynamic results. It is found in the range of 0.3 - 0.4. The generalized forces and torques for both links therefore become

$$F_{dt} = \sum_{i=1}^2 \left(\frac{\partial^0 \omega_i}{\partial \dot{\theta}_t} . T_{di} + \frac{\partial^0 v_i}{\partial \dot{\theta}_t} . R_{di} \right) \quad (37)$$

2.2.6 Control forces and Servo motor Dynamics :

Present system is under-actuated as two 1 DOF rotational joint actuators and a ballast system are utilized as control inputs to provide the planar forward motion and diving-in/out operation. The head is connected to the caudal tail using rotational joint about z axis, the torque for which is given by

$$T_i = T_i \hat{z}_{i-1} \quad (38)$$

In a DC motor equation with standard notation [4,9], torque T_i is a function of angular rotational velocity ω_m and armature voltage V_a given by

$$T_i = f(\omega_m, V_a) \quad (39)$$

where armature voltage V_a is

$$V_a = \frac{r_a}{K_m} \tau_m + K_e \dot{\theta}_m \quad (40)$$

τ_m is motor torque then T_i can be written as

$$T_i = f(\omega_m, \tau_m) \quad (41)$$

The generalized active control force is expressed as

$$F_c = \frac{\partial^0 \omega_i}{\partial \dot{\theta}_t} . T_0 + \frac{\partial^0 v_i}{\partial \dot{\theta}_t} . R_0 + \sum_{i=1}^2 \left(\frac{\partial^0 \omega_i}{\partial \dot{\theta}_t} .^0 A_i . T_i \right) \quad (42)$$

2.3 Equation of Motion in Earth fixed coordinates

The forces and moments for the complete system in body fixed coordinate i.e. robotic fish head and caudal tail are determined comprising of generalized inertia forces, generalized active forces and generalized Lighthill reactive forces for the carangiform fish type design. Equating (12), (33), (36), (39) and (44) to write a force balance equation as:

$$F_i + F_{LH} + F_b + F_d + F_c = F_{tail} \quad (43)$$

As proposed in this paper, the anterior head motion in space is propelled by the cumulative thrust forces and balancing moments generated from the posterior 2-link assembly, equating (3) and (46) to obtain the unified system(vehicle) motion equation in body fixed coordinate(subscript vb) as

$$M_{vb}(\zeta) \dot{\zeta} + C_{vb}(q, \zeta) \zeta + D_{vb}(q, \zeta) \zeta + g_{vb}(q, \eta) = F_{tail}^{[vb]} \quad (44)$$

where $\zeta = [\nu^T, \dot{q}^T]^T$ where

$$M_{vb}(\zeta) = \begin{bmatrix} (M_h + m) & 0 \\ 0 & M_t(q) \end{bmatrix}$$

$$C_{vb}(q, \zeta) = \begin{bmatrix} C_h(\nu) & 0 \\ 0 & C_t(q, \dot{q}) \end{bmatrix}$$

$$D_{vb}(q, \zeta) = \begin{bmatrix} D_h(\nu) + & 0 \\ 0 & D_t(q) \end{bmatrix}$$

$$g_{vb}(q, \eta) = \begin{bmatrix} g_h(\eta) \\ g_t(q) \end{bmatrix}$$

It can be noted that as off-diagonal elements are smaller in magnitude compared to the diagonal elements, they have been reduced to zero. Kinematic Transformation [4, 16] is undertaken to convert the system from body fixed coordinate $[\nu, \dot{q}]$ to earth fixed coordinate $[\eta, \dot{x}_t]$ by defining the relation using Jacobian matrix J for fish head and caudal tail.

a) Fish Head

Body fixed vector ν and earth fixed vector η are equated [4] by

$$\dot{\nu} = J_R^{-1}(\eta) [\ddot{\eta} - \dot{J}_R(\eta) J_R^{-1}(\eta) \dot{\eta}] \quad (45)$$

where

$$J_R(\eta)_{6 \times 6} = \begin{bmatrix} J_1(\eta_2) & 0_{3 \times 3} \\ 0_{3 \times 3} & J_2(\eta_2) \end{bmatrix}$$

with

$$J_1(\eta_2) = \begin{bmatrix} c\psi c\theta' & -s\psi c\phi + c\psi s\theta' s\phi & s\psi s\phi + c\psi c\phi s\theta' \\ s\psi c\theta' & c\psi c\phi + s\psi s\theta' s\phi & -c\psi s\phi + s\theta' s\psi c\phi \\ -s\theta' & c\theta' s\phi & c\theta' c\psi \end{bmatrix}$$

and

$$J_2(\eta_2) = \begin{bmatrix} 1 & s\phi t\theta' & c\phi t\theta' \\ 0 & c\phi & s\phi \\ 0 & s\phi/c\theta' & c\phi/c\theta' \end{bmatrix}$$

where ψ = yaw (heading) angle, θ' = pitch angle and ϕ = roll angle of the vehicle.

b) Caudal tail

The tail-fin x_t position in cartesian space is related to joint variable q [9] by

$$\dot{q} = J_2^{-1}(\eta) [\dot{x}_t - J_1 J_R^{-1}(\eta) \dot{\eta}] \quad (46)$$

For the two link manipulator the jacobian matrix is given by

$$J = \begin{bmatrix} -(l_1 s\theta_1 + l_2 s\theta_{12}) & -l_2 s\theta_{12} \\ l_1 c\theta_1 + l_2 c\theta_{12} & l_2 c\theta_{12} \\ 0 & 0 \\ 0 & 0 \\ 0 & 0 \\ 1 & 1 \end{bmatrix}$$

Putting in equation (46) the unified dynamic equations of motion of robotic fish vehicle in earth fixed coordinate (subscript *vh*) is written as

$$M_{ve}(q, \eta, \zeta)\ddot{\xi} + C_{ve}(q, \eta, \zeta)\dot{\xi} + D_{ve}(q, \eta, \zeta)\xi + g_{ve}(q, \eta) = F_{tail[ve]} \quad (47)$$

where $\xi = [\eta^T, x_t^T]^T$

$$M_{ve} = J^{-T}(q, \eta)M(q)J^{-1}(q, \eta) \quad (48)$$

$$C_{ve} = J^{-T}(q, \eta)[C(q, \zeta) - M(q)J^{-1}(q, \eta)\dot{J}(q, \eta)]J^{-1}(q, \eta) \quad (49)$$

$$D_{ve} = J^{-T}(q, \eta)D(q, \zeta)J^{-1}(q, \eta) \quad (50)$$

$$g_{ve} = J^{-T}(q, \eta)g(q, \eta) \quad (51)$$

$$\tau_{ve} = J^{-T}(q, \eta)\tau \quad (52)$$

where

$$J(q, \eta) = \begin{bmatrix} J_R(\eta) & 0 \\ J_1(\eta) & J_2(q) \end{bmatrix}$$

3. SIMULATION AND EXPERIMENT RESULTS DISCUSSION

Simulations and experiments for this unified model is limited to a straight path as done in realtime experiments with biological fishes with a good estimation that vital relative motions of posterior body (responsible for thrust) are in lateral direction. Project implementation is done in MATLAB and Simulink. The yaw-axis servomotor is a Hitec HS-5646WP (11.3Kgcm/6 V) used in the two joints. Arduino-Uno with ATMEGA328P serves as central processing unit for the robotic fish. A comprehensive kinematic study of the different parameters namely tail-beat frequency (TBF), propulsive wavelength, yaw angle and caudal amplitude are studied under this framework [20,21]. TBF is found to be the effective controlling parameter for the forward speed of the vehicle over a wide operating region. LH algorithm is integrated with robotic fish dynamics model proposed in this paper implemented in open loop. Based on the present dynamic model and steady simulation results [20,21], the open-loop (manual) experimental validations were done to mimic the undulation of the robotic fish caudal tail in fluid environment shown in Fig.4. Different undulatory modes of caudal fin is shown in this figure to achieve a rectilinear locomotion pattern. Based on the experiments an operating region plot of forward swimming velocity in cm/sec (vertical axis) and TBF in Hz (horizontal axis) is shown in Fig 5(a). Range of TBF is from 0 - 2.8 units (Hz) [21] while for wavelength it is 1.2 - 2.2 units (cm)[20]. Variation of swimming speed with TBF and wavelengths are shown as oscillating bell shaped curves. Peaks marked by a star symbol show maximum velocities achieved at TBF values of 0.5 Hz, 0.75 Hz and 1.1 Hz at constant wavelength values of 1.1 cm, 1.2 cm and 1.3 cm respectively, highest being 17.3 cm/sec at 1.1 Hz. Fig.5(a) shows a peak velocity of 17.28 cm/sec at a wavelength (1.45 cm) and TBF of 0.5 Hz. Therefore, for any choice of speed (based on the purpose like fast or moderate swimming) the combinational choice of two parameters (TBF and wavelength) can be found for operating robotic fish. Interestingly, it can be observed that many times, for a given velocity there exists two or more values of TBF. This is due to the non-linear

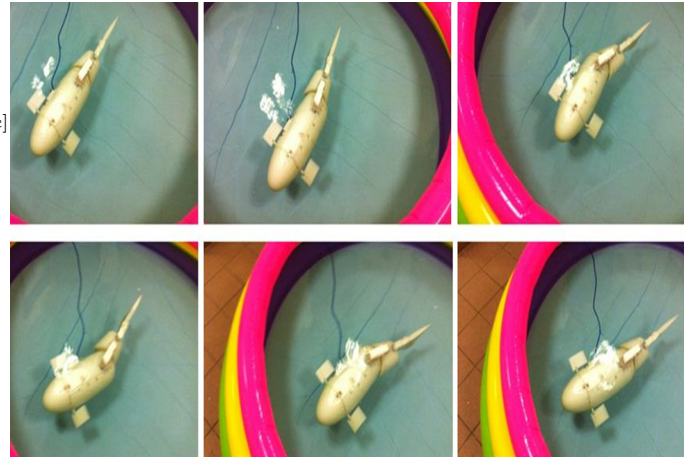
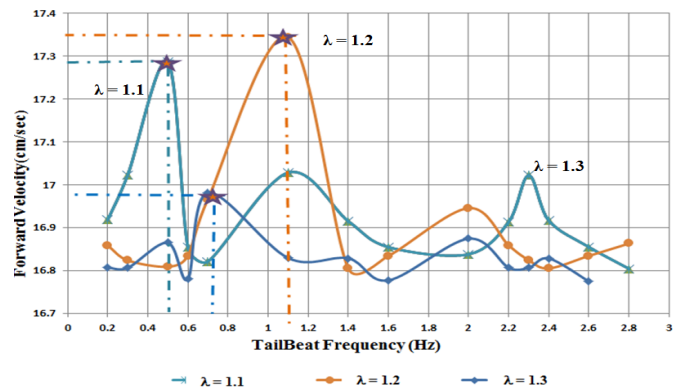
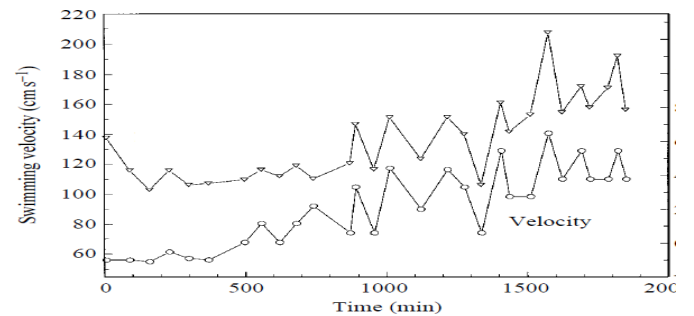


Fig. 4. Open-loop Hardware prototype motion in different swimming modes

nature of the bell-curve function mapping. Value of caudal amplitude is kept constant at $c_1 = 0.002$ and $c_2 = 0.00835$ [20]. Interestingly these plots, are identical to their biological counterpart mentioned by Dewars experiment[14] on yellowfin tuna kinematics shown in Fig. 5(b).



(a) Operating Region for Robotic fish using Forward velocity and TBF



(b) Dewar's Experimental Result of Swimming(forward) Velocity vs time for a yellowfin tuna

Fig. 5. Kinematic Experimental Results

4. CONCLUSION

Present paper develops a unified bio-harmonized dynamic model of a bio-inspired robotic fish underwater vehicle based on Lighthill's (LH) Slender Body theory. Firstly, the rigid body dynamics for the head (anterior) of the robotic fish is defined. The posterior caudal-tail is designed to be a 2-link serial manipulator whose equations of

motion including the inertial and hydrodynamic forces are developed based on Kane's methodology. The added mass inertia forces and torques are integrated as reactive and balance side-forces respectively, mentioned in the bio-fluid-dynamics of carangiform fish motion in Lighthill's slender body theory. This two way bio-mechanism is used by piscine species to maximize their thrust while swimming and reducing the unbalance caused by the undulatory motion of caudal tail. The proposed Lighthill reactive forces added with other generalized inertia and active forces account for caudal-tail thrust. During robotic fish caudal tail undulatory motion, LH reactive forces generate the inertial added mass. A unified non-linear equation is developed to drive the robotic fish head dynamic motion balanced by the caudal-tail generated thrust. Based on this unified dynamic model, the system performance is evaluated for identified major kinematic parameter *TBF*. Based on proposed unified dynamic model simulation of identified kinematic parameters open-loop experiments are done and *TBF* operating region is established. Robot kinematic swimming results are found to be matching that of a biological yellow fin tuna kinematics experimental studies.

ACKNOWLEDGEMENTS

We would like to thank Mr. Alok Agrawal of Purdue University for key contributions for the mechanical CAD design of Robotic fish. We would acknowledge useful suggestions and feedback given by Mr. Shailabh Suman of Acoustic Research Lab NUS, Dr. Mandar Chitre of Acoustic Research Lab NUS, Dr. Pablo Alvaro Valdivia of Singapore-MIT Alliance for Research and Technology (SMART), Professor Marcelo H. Ang Jr. and Professor Xu Jianxin of Department of Electrical and Computer Engineering.

REFERENCES

- [1] M. S. Triantafyllou, A. H. Techet, and F. S. Hover, Review of experimental work in biomimetic foils. *IEEE J. Ocean. Eng.*, Volume 29, no. 3, pages 585-594, Jul. 2004.
- [2] P. R. Bandyopadhyay, Trends in biorobotic autonomous undersea vehicles. *IEEE J. Ocean. Eng.*, Volume 30, no. 1, pages 109-139, Jan. 2005.
- [3] P. W. Webb, Form and function in fish swimming. *Scientific American*, Volume 251(1), pages 58-68, 1984.
- [4] Fossen, T. I. (2011). Handbook of Marine Craft Hydrodynamics and Motion Control. *John Wiley & Sons Ltd.* Hardcover: ISBN 978-1-1199-9149-6, Kindle: available at www.amazon.com
- [5] Schjolberg, I. and Fossen, T.I. Modelling and control of underwater vehicle-manipulator systems. In: Proc. of the 3rd Int. Conf. on Manoeuvring and Control of Marine Craft. Southampton, England, 1994.
- [6] T. J. Tarn, G. A. Shoults, S. P. Yang, A dynamic model of an underwater vehicle with a robotic manipulator using Kane's method. *Journal of Autonomous Robots*, Volume 3, Issue 2-3, pages 269-283, 1996
- [7] Nakashima, Motomu; Ohgishi, Norifumi; Ono, Kyosuke, A Study on the Propulsive Mechanism of a Double Jointed Fish Robot Utilizing Self-Excitation Control. *JSME International Journal Series C*, Volume 46, Issue 3, pages 982-990, 2003.
- [8] Barrett D., Grosenbaugh M., and Triantafyllou. The Optimal Control of a Flexible Hull Robotic Undersea Vehicle Propelled by an Oscillating Foil. *Proceedings of the IEEE Symposium on Autonomous Underwater Technology*, Monterey, CA, pages 1-9, 1996.
- [9] Junzhi Yu and Long Wang. Design Framework and 3-D Motion Control for Biomimetic Robot Fish. *IEEE International Symposium on Intelligent Control*, pages 1435-1440, Cyprus, 2005.
- [10] Lighthill, M. J. Note on the swimming of slender fish. *Journal of Fluid Mechanics*. Volume 9, pages 305-317, 1960.
- [11] Jianxun Wang, Freddie Alequin-Ramos, Xiaobo Tan. Dynamic modeling of robotic fish and its experimental validation. *IEEE/RSJ International Conference on Intelligent Robots and Systems*, pages 25-30, San Francisco, CA, USA, 2011
- [12] Lighthill, M. J. Large-amplitude elongated-body theory of fish locomotion. *Proc. R. Soc. Lond. B* Volume 179, pages 125-138, 1971.
- [13] Lighthill, M. J. Aquatic animal propulsion of high hydrodynamic efficiency. *Journal of Fluid Mechanics*. Volume 44, pages 256-301, 1970.
- [14] H Dewar, J Graham. Studies of Tropical Tuna Swimming Performance in a Large Water Tunnel - Kinematics. *Journal of Experimental Biology*. Volume 192, Issue: 1, pages 45-59, 1994.
- [15] Kane, T.R., Likens, P.W., and Levinson, D.A. *Spacecraft Dynamics*. McGraw-Hill Inc. 1983.
- [16] Fu K.S, R.C Gonzalez, and C.S Lee. *Robotics Control, Sensing, Vision and Intelligence*. New York: McGraw-Hill. 1987.
- [17] K. H. Low, C. W. Chong, Chunlin Zhou, and Gerald G. L. Seet. An Improved Semi-Empirical Model for a Body and/or Caudal Fin (BCF) Fish Robot. *IEEE International Conference on Robotics and Automation* pages 78-83, Anchorage 2010.
- [18] Boyer, F., Porez, M., Leroyer, A., and Visonneau, M. Fast dynamics of an eel-like robot - comparisons with Navier-Stokes simulations. *IEEE Transaction on Robotics*, Volume 24, pages 1274-1288, 2008.
- [19] Junzhi Yu, Min Tan, Shuo Wang, and Erkui Chen. Development of a Biomimetic Robotic Fish and Its Control Algorithm, *IEEE Transactions On Systems, Man, And Cybernetics Part B: Cybernetics*, Volume 34, No. 4, 2004.
- [20] Chowdhury Abhra Roy, Prasad. B; Vishwanathan. V; Kumar. R; Panda. S. K. Kinematics study and implementation of a biomimetic robotic-fish underwater vehicle based on Lighthill slender body model. *IEEE/OES Autonomous Underwater Vehicles (AUV)*, pages 1-6, National Oceanography Centre Southampton UK, 2012.
- [21] Chowdhury Abhra Roy, Prasad. B; Vishwanathan. V; Kumar. R; Panda. S. K. Implementation of a BCF Mode Bio-mimetic Robotic Fish Underwater Vehicle based on Lighthill Mathematical Model. *IEEE RAS ICROS International Conference on Control, Automation and Systems (ICCAS)*, pages 437-442, Korea, 2012.